Molecular grafting can generate bioactivities within the cyclic peptide PDP-23

Fatemeh Hajiaghaalipour,[1] Angela Song,[1] Grishma Vadlamani,[2] Jingjing Zhang,[2] Joshua S. Mylne,[2,3] Richard J. Clark[1] and K. Johan Rosengren[1*]

[1]The University of Queensland, School of Biomedical Sciences, Brisbane, QLD 4072, Australia
[2]The University of Western Australia, School of Molecular Sciences, Crawley, WA 6009, Australia
[3]Curtin University, Centre for Crop and Disease Management, School of Molecular and Life Sciences, Bentley, WA 6102, Australia
[*]Address correspondence to: K. Johan Rosengren, The University of Queensland, School of Biomedical Sciences, St Lucia QLD 4072, Australia. E-mail: j.rosengren@uq.edu.au; Phone: +61 7 3365 1403

Abstract

The stability of cyclic peptides, coupled with their structural diversity and ability to host an extensive range of bioactivities, make them promising leads for the development of new drugs. PawS-Derived Peptide-23 (PDP-23) is a head-to-tail macrocyclic peptide with two disulfide bonds produced in plant seeds. Its unusual fold comprises two β-hairpins connected by hinges that allow the structure to adapt to different environments. In water two PDP-23 molecules form a compact intertwined dimer that buries hydrophobic residues, whereas in membrane mimicking conditions it adopts an open monomeric form that expose them. Here we investigate PDP-23 as a novel scaffold for the grafting of bioactive epitopes and conjugation of small molecules. To explore the plasticity of PDP-23 we introduced the bioactive loop of sunflower trypsin inhbitor-1 (SFTI-1) or an integrin binding RGD motif into either of the β-hairpins. Solution NMR spectroscopy revealed that although the variants were unable to dimerise, the structural features of both the graft and scaffold were retained. SFTI-1 hybrid variants showed trypsin inhibitory activity. PDP-23 has previously been used as a cell permeable drug scaffold targeting drug-resistant cancer cells by inhibiting the drug efflux pump P-glycoprotein and restoring their sensitivity to chemotherapeutic. Introducing the RGD motif into such PDP-23 conjugates significantly improve their potency, suggesting that the RGD sequence targets the peptide to the membrane of cancer cells and improve cell uptake. In conclusion, this study highlights PDP-23 as a stable and versatile scaffold for molecular grafting of bioactivities and targeted delivery of pharmaceutical payloads.

Keywords: PawS-Derived Peptide, PDP-23, grafting, SFTI-1, trypsin inhibition, RGD, peptide-drug conjugate, cancer resistance, multidrug exporter, P-glycoprotein (P-gp)

Currently used drugs can generally be split into two major classes based on size; small molecule drugs with typical molecular weight of <500 Da and larger biologics typically >5000 Da. Peptides, containing fewer than 50 amino acids, fill a space between biologics and small molecules, and are able to incorporate benefits from each category.[1, 2] They can create a range of intermolecular contacts that allow for more selective interactions than small molecules but retain advantages over biologics in terms of cell and tissue permeability. Since the discovery of insulin as the first therapeutic peptide in 1921 the field has seen tremendous progress, with more than 80 peptide drugs approved for use around the world.[2, 3] The structural and functional diversity of cyclic peptides make them particularly interesting leads for the development of more effective and stable drugs. Features such as disulfide bonds and a cyclic backbone serve as cross-links that stabilize the structure of peptides, preventing chemical and biological breakdown. Consequently, cyclic peptide research has become an increasingly important area of drug design.[3-6]

Numerous studies have highlighted the clinical potential of natural product macrocycles and their synthetic derivatives over the past decades. Disulfide-rich macrocyclic peptides have been shown to be amenable to molecular grafting.[7] The term "grafting" in this context refers to the process of inserting a small peptide epitope with desirable activity into a framework to provide it with increased stability and properties. Many macrocyclic peptides from plants have been used as grafting scaffolds. Kalata B1 from the Möbius subfamily of cyclotides was the first engineered cyclotide,[8] and has, among other things, been grafted with a peptide epitope involved in VEGF-A antagonism to generate antiangiogenic activity against VEGFR2 as a potential cancer therapy.[9] Another scaffold frequently used for peptide engineering is sunflower trypsin inhibitor-1 (SFTI-1), which comprises 14 amino acids with one disulfide bond and a cyclic backbone. SFTI-1 is naturally a potent trypsin inhibitor, which was discovered in seeds of the common sunflower *Helianthus annuus*.[10] SFTI-1 has been used as a stable framework for grafting bioactive peptides, for sequence mutagenesis to alter protease inhibitor selectivity, and as a model peptide for evaluating peptidomimetic motifs and platform technologies.[11] From the perspective of therapeutic potential SFTI-1 has been explored in the areas of autoimmune disease,[12, 13] chronic inflammatory disorders,[14] cancer,[15] cardiovascular,[16] and obesity.[17]

SFTI-1 is the prototypic member of the Paws-Derived Peptide (PDP) family, which currently has 24 members, all produced in seeds from the Asteraceae family. Genetically they are

encoded as inserts in seed storage albumins that are post-translationally excised and cyclized during the processing of the albumin preprotein.[18] The most recently discovered members, PDP-23 and PDP-24, are unique in that they are twice the size of SFTI-1 and comprise two disulfide bonds.[19-21] NMR spectroscopy studies have shown that PDP-23 adopts a dimeric structure in which each monomer comprise two hairpins that come together in a square-prism shape enclosing a substantial hydrophobic core.[19] In the presence of organic co-solvents PDP-23 dissociates into well-defined 'V'-shaped monomeric forms, while in membrane mimicking micelles it opens up fully to expose a hydrophobic patch to the membrane environment. Furthermore, PDP-23 can internalize into cells, and has been shown to act as an inhibitor of P-glycoprotein (P-gp) after conjugation of a rhodamine analogue that is a known substrate of this drug exporter. Importantly, this inhibition of P-gp can restore sensitivity of resistant cancer cells towards common chemotherapeutics.[19] PDP-24 is unable to form a dimeric structure, but adopts a similar structure to PDP-23 in organic co-solvent, highlighting that these types or PDPs share the common feature of stable hairpins linked by flexible hinges that are able to rearrange their relative positions.[20]

Currently, increased attention has been focused on the usefulness of peptides as a targeted ligand for the effective treatment and diagnosis of cancer cells.[22-24]r The expression of several molecular receptors on the endothelial cell surface in tumor blood vessels, can be used to distinguish them from the vasculature of other normal cells and tissues.[25] The tripeptide arginine-glycine-aspartic acid (Arg-Gly-Asp or RGD), an integrin binding motif, was discovered to be the minimal cell-recognizable sequence in numerous blood and extracellular matrix proteins in the 1980s.[26] Peptide ligands containing RGD triad can be conformationally tuned to be selective for different integrins, with the $\alpha_V\beta_3$ integrin receptor variant being a primary target as many tumor-associated cells that expressing this receptor.[25] Specific delivery of chemotherapeutics to malignant tissues increase the efficacy of cytotoxic components and limit the peripheral toxicity.

The unique structural, biopharmaceutical properties, ultrastability, and diverse design possibilities make it likely that the cyclic disulfide-rich peptides will play an even more important role in the future, and this research aims to explore opportunities for drug discovery using the novel PDP-23. We hypothesised that PDP-23 is an ideal peptide scaffold for protein engineering because of its high resistance to thermal, enzymatic, and chemical degradation, coupled with its unique ability to adopt different structures in different environments.

Therefore, we investigated the ability of PDP-23 to host different epitopes to infer biological activities. We show the PDP-23 scaffold can tolerate SFTI-1 and RGD grafts and accommodate both trypsin inhibition and protein-protein interaction activities.

Methodology

Peptide synthesis, cyclisation, folding and purification

PDP-23 analogues were synthesized on 2-chlorotrityl chloride resin at a 0.5 mmole scale by Fmoc-based solid phase peptide synthesis using a CS336X automated peptide synthesizer (CSBio, CA, USA). Peptides were synthesized starting with Gly1 to generate a C-terminal Gly for cyclisation. Gly1 was therefore protected with 2,4-dimethoxybenzyl to minimize the risk of isoaspartamide formation due to the next residue being and Asp. After peptide assembly the N-terminal Fmoc group was removed by adding 20% piperidine in dimethylformamide (DMF). Upon completion of synthesis, the peptide was cleaved from resin with 1% trifluoroacetic acid (TFA) in dichloromethane (DCM) to maintain sidechain protection of amino acids. Acetonitrile (ACN) was added and the solution was rotary evaporated to remove the DCM and TFA before lyophilisation.

The peptide, at a concentration of 2 mM in DMF, was then cyclized by adding 1 eq. of 1-[Bis(dimethylamino)methylene]-1H-1,2,3-triazolo[4,5-b]pyridinium 3-oxide hexafluorophosphate (HATU), followed by DIPEA (10 eq.). The reaction was monitored by electrospray mass spectrometry (ESI-MS) over 6 h by dilution of a sample of the cyclization mixture in 50:50 ACN/H_2O prior to direct injection. After cyclisation the peptide was extracted from the DMF using phase extraction with DCM. ACN was added to the DCM/peptide solution prior to rotary-evaporation of the DCM followed by lyophilization.

Deprotection of sidechains was conducted by addition of 50 mL of a solution containing TFA, triisopropylsilane (TIPS), 3,6-dioxa-1,8-octanedithiol (DODT) and water (92:5: 2.5: 2.5: 2.5). After 2 h stirring, the TFA was evaporated via rotary-evaporation and the peptide precipitated from the solution using cold diethyl ether. The precipitated peptide was filtered and re-dissolved in a solution of ACN/H_2O (50:50) before lyophilization. Crude peptide was purified via reverse phase high performance liquid chromatography (RP-HPLC) using buffer A (0.05% TFA in water) and buffer B (90% ACN, 0.05% TFA in water) at a gradient of 1%/min on a preparative C18 column (300 Å, 10 μm, 21.20 mm i.d x 250 mm, Phenomenex). Electrospray ionization mass spectrometry (ESI-MS) was used to confirm the molecular mass of the peptide.

Disulfide bond formation between cysteine residues in all PDPs was achieved using regioselective disulfide bond formation with acetamidomethyl (ACM) and trityl (Trt)-protected Cys residues protected cysteine residues. The formation of the first disulfide bond, between cysteines liberated from their Trt protecting groups during general sidechain deprotection was formed by dissolving the peptide in 0.1 M ammonium bicarbonate at a concentration of 0.25 mg/ml with 2 mM reduced glutathione, pH 8.3, and stirring for 24 h. After this buffer A was added as well as drops of TFA to decrease the pH to 6 prior to further purification using a semi-preparative C18 column (300 Å, 5 µm, 10 mm i.d. x 250 mm, Vydac) with a 1% gradient of buffer A and buffer B and a flow rate of 8 mL/min.

The removal of the ACM protecting groups and formation of the second disulfide bond was conducted via iodolysis in buffer A at a concentration of 0.25 mg/mL. A pre-prepared solution of 0.1 M iodine in buffer A/buffer B (50:50) was added to the peptide solution until a noticeable color change from clear to orange was achieved. This solution was then stirred under nitrogen in a dark environment for 2 h, prior to quenching with ascorbic acid. Final purification was conducted using the above method, and purity was determined using RP-HPLC with a C18 analytical column (300 Å, 5 µm, 2.1 mm i.d. x 150 mm, Vydac). Electrospray Ionization Mass Spectrometry (ESI-MS) confirmed the molecular mass of the fully oxidized peptides. Analytical RP-HPLC and MS data for final peptides are provided as Supporting Information (Figures 1-3).

NMR spectroscopy

To monitor structural changes of the scaffold and the conformation of the introduced epitopes structural studies were performed using solution NMR spectroscopy. For NMR studies peptide samples were made up with ~1 mg peptide in a 500 µL solution of either (90:10) H_2O/D_2O or $H_2O/D_2O/CD_3CN$ (70:10:20) at pH ~ 3.5. NMR data were recorded at 700 or 900 MHz on Bruker Avance III spectrometers equipped with cryo-probes. A range of spectra were recorded, including 1D ^1H, 2D ^1H-^1H TOCSY (Total Correlation Spectroscopy) with a mixing time of 80 ms, and ^1H-^1H NOESY (Nuclear Overhauser Spectroscopy) with a mixing time of 200 ms, which allowed complete ^1H resonance assignment using sequential assignment strategies.[27, 28] Data were referenced to the solvent signal (4.77 ppm for H_2O in aqueous samples and 2.031 ppm for residual protons in samples containing CD_3CN). Secondary ^1H Hα chemical shifts were calculated using established random coil shifts.[29]

Trypsin inhibition assays

Inhibition of trypsin was tested using established assays as described.[30] Synthetic peptides were dissolved and assayed for inhibitory activity in a buffer composed of 50 mM Tris-HCl (pH 7.8) and 20 mM calcium chloride for 15 min at 37 °C. Serially diluted peptide stock (5 µL) was added to 20 µL of a 25 µg/mL solution of trypsin from bovine pancreas (Sigma-Aldrich) to generate final concentrations ranging from 0.01 to 1 µM. Then 1 mM N-α-benzoyl-l-arginine-p-nitroanilide substrate (Sigma-Aldrich) was added to initiate the reaction and incubated for 30 min at 37 °C. All reactions were performed in triplicate, and soybean Bowman–Birk inhibitor (Sigma-Aldrich) was used as a positive control. The trypsin activity of reaction wells with no inhibitor/peptide present was designated as 100%, and the inhibitory activity of synthetic peptides was determined in relation to the no-inhibitor controls. After the incubation time, the reaction was stopped by adding 25 µL of 30% (v/v) acetic acid and the absorbance was measured at 410 nm.

Cell culture and cell cytotoxicity assays

The HeLa cervical cancer cell line was used to evaluate the toxicity of the grafted peptide analogues. The cells were cultured in Eagle's minimum essential medium, supplemented with 10% fetal bovine serum (FBS) and 50 U/mL of penicillin and 50 mg/mL streptomycin. The cells were incubated in a humidified atmosphere containing 5% CO_2 at 37 °C. The cell toxicity of the RGD grafted PDP-23 analogues were evaluated by 3-(4,5,-dimethyl-2-thazolyl)-2,5-diphenyl-2H-tetrazolium bromide (MTT) assay as described previously.[31].

Peptide labelling

The conjugation of 5/6-carboxy-tetramethyl-rhodamine to the PDP-23 D28K analogue and RGD grafted PDP-23 D28K was conducted by dissolving of ~5 mg, of the peptide in 0.1 M sodium phosphate at a concentration of 1 mg/mL adjusted to pH 8.75. Then a pre-prepared solution containing 10 molar equivalents of NHS-5/6-carboxy-tetramethyl-rhodamine at a concentration of 10 mg/mL in DMSO was added to the peptide solution and stirred overnight at room temperature protecting from light. The conjugation solution was diluted 10-fold prior to repurifying the peptide-drug conjugate by using RP-HPLC. Analytical RP-HPLC and MS data for the PDP-23-5/6-carboxy-tetramethyl-rhodamine and the grafted PDP-23-5/6-carboxy-tetramethyl-rhodamine (RGD and RGDΔH) are provided as Supporting Information (Figures 4-5).

Cell culture and daunorubicin sensitivity assays

Daunorubicin and verapamil were dissolved in DMSO and then were diluted in the Dulbecco's Modified Eagle Medium (DMEM) medium to make working stocks, with the final solvent concentration <1%. The RGD grafted analogues of PDP-23-5/6-carboxy-tetramethyl-rhodamine were reconstituted in DMEM to a concentration of 30 μM, which was further diluted to produce working stocks.

KB-3-1 (sensitive) and KB-V-1 (resistant) cells were grown in DMEM medium, supplemented with 10% FCS, and 100 μg/mL penicillin/streptomycin at 37 °C with 5% CO_2. Cells were seeded in a 96-well plate at a density of 10,000 cells per well in 100 μL of DMEM medium and incubated overnight at 37 °C. Then, the cells treated with PDP-23-RGD grafted analogues-rhodamine conjugate at concentrations of 1, 5, 10 or 30 μM supplemented with 1 μM daunorubicin. for 24 h. Cells were additionally treated with positive controls of 30 μM verapamil supplemented with 1 μM daunorubicin, as well as daunorubicin 1 μM alone. Untreated cells, as well as cells treated with 30 μM verapamil only, were included as negative controls.

Toxicity was assessed using the CyQuant NF Proliferation assay according to manufacturer's protocol (CyQuant NF Proliferation assay kit). After incubation, medium was removed, and cells incubated with the DNA-binding fluorescent dye reagent (CyQuant NF Proliferation assay kit) in Hank's Balanced Salt Solution for 30 min at 37 °C. Fluorescence was measured at 485 ex/520 em. Data were normalized to the untreated control.

Results and Discussion

Peptide Design: Targeting trypsin and $\alpha_V\beta_3$ integrin by grafting into PDP-23

The structural tolerance of substitutions in the PDP-23 framework was first investigated by grafting of the bioactive loop of SFTI. The conformation of this loop is similar to the loops at both ends of PDP-23 in that it is restrained by a disulfide bond that stabilizes a β-hairpin. Consequently, we chose to retain the PDP-23 disulfide bridged core but replaced either the Trp^4-His^5-His^6-Ser^7 or the Ala^{15}-Asp^{16}-Phe^{17}-Pro^{18}-Trp^{19}-Pro^{20}-Leu^{21}-Gly^{22}-His^{23}-Gln^{24} segments of PDP-23 with the trypsin inhibitory sequence Thr-Lys-Ser-Ile-Pro-Pro-Ile from SFTI-1 (Figure 1). By lining up the disulfide of SFTI-1 with either disulfide of PDP-23, all of which adopt a right handed staple conformation,[19, 32] we expected that the correct shape of the bioactive loop could be retained, thereby introducing trypsin inhibitory activity to PDP-23.

Furthermore, the concept of using PDP-23 as drug scaffold was evaluated by inserting an Arg-Gly-Asp (RGD) sequence into loop 1 of PDP-23. RGD sequences are among the most studied short sequences that mediate protein-protein interactions,[33, 34] and have been widely used in proof-of-concept sequences for molecular grafting.[35, 36] Specific targeting of $\alpha_V\beta_3$ integrin is a promising approach for targeted cancer therapy given that its over expression on many cancer cells.[37, 38] Here we chose to either insert the RGD segment between His^5-His^6 or replacing His^6 with RGD, resulting in a seven or six residue loop, respectively (Figure 1). The altered loop length may affect the conformation of the RGD segment, potentially influencing integrin binding.

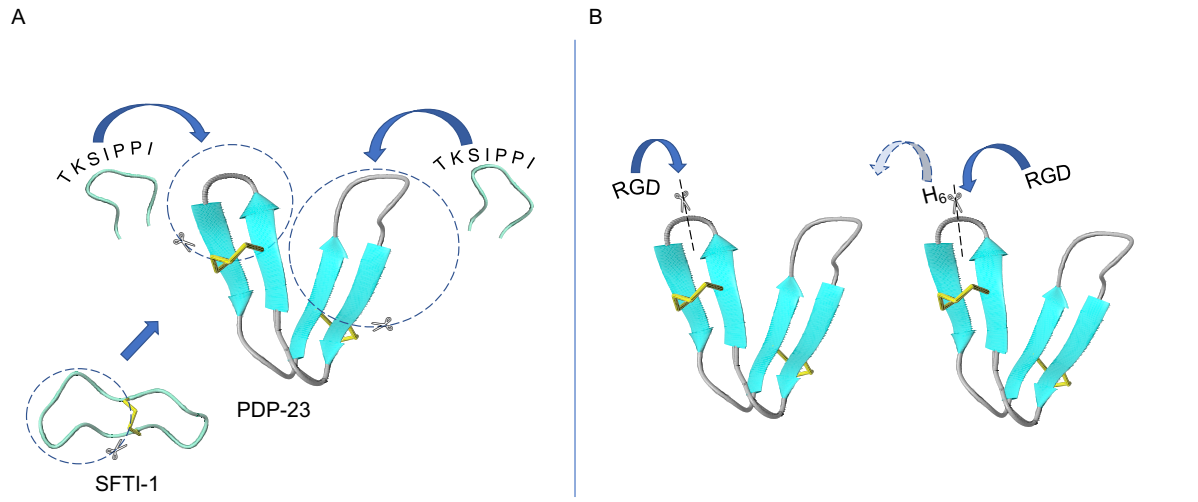

C

Peptide	Amino acid sequence and disulfide bonds
PDP23	GFC3 W H H S C8 VPSGTC14 ADFPWPLGHQC25 FPD
PDP23-SFTI-loop1	GFC3 T K S I P PIC11 VPSGTC17 ADFPWPLGHQC28 FPD
PDP23-SFTI-Loop2	GFC3 W H H S C8 VPSGTC14 T K S I P P I C22 FPD
PDP23-RGDΔH	GFC3 WH R G D SC10 VPSGTC16 ADFPWPLGHQ C27 FPD
PDP23-RGD	GFC3 WHRGDHSC11 VPSGTC17 ADFPWPLGHQ C28 FPD

Figure 1. Grafting of bioactive sequences into PDP-23. (A) Structure of PDP-23 illustrating the two hairpins and the insertion of the bioactive loop of SFTI-1. (B) Structure of PDP-23 illustrating the insertion of the RGD epitope in loop 1. (C) Sequences of PDP-23 and analogues designed and characterized in this study.

Peptide synthesis and NMR spectroscopy

Solid-phase Fmoc chemistry, cyclization in solution, and oxidization by regioselective disulfide formation were used to synthesize PDP-23 and analogues. Each peptide was purified by RP-HPLC and the ratio of their mass to charge (m/z) confirmed by ESI-MS, showing that the incorporation of the SFTI-1 or RGD sequences can easily be achieved using our synthetic methodology. To determine whether the structural characteristics of the scaffold are maintained in the grafted peptides, structural characterization of the grafted peptides were carried out solution NMR spectroscopy. Initially, data for all peptides were recorded in water, conditions under which native PDP-23 is dimeric. Strikingly all variants, showed poor quality NMR data, with very broad resonance lines, suggesting significant aggregation. This finding suggests the grafts destabilize the dimer and the peptide exist in interconverting structural forms in solution. This is consistent with what was observed for PDP-24 in water. Despite only five amino acid substitutions relative to PDP-23, PDP-24 is not able to adopt a well-defined dimer,[20] possibly

because it lacks one amino acid in the hinge region between the β-sheets, preventing them from lining up appropriately. We then rerecorded all data in the presence of 20% ACN and, as for PDP-24, this significantly improved the quality of data, with all analogues giving sharp lines and good resonance dispersion suggesting a structured fold. Notably downfield shifted Hα resonances were observed as expected for β-sheet containing peptides. Two dimensional TOCSY and NOESY data were recorded and allowed complete resonance assignment of the peptide backbone and most side chains. To compare the structural features of the analogues with native PDP-23 and native SFTI-1 we determined the secondary Hα chemical shifts, which are highly sensitive to secondary structure.[29]

The secondary Hα chemical shifts of SFTI and RGD grafted PDP-23 (Figure 2) show the structural features of the scaffold are closely retained, with the trends and magnitudes of the secondary shifts matching native PDP-23 in the regions that have not been modified. Moreover, the secondary shifts of the SFTI-1 graft sequence itself closely matches that of native SFTI-1, including the large positive values of the cysteine residues at positions 3 and 11 in the loop 1 graft and positions 14 and 22 in the loop 2 graft. Some differences are seen around the 'hinge' regions between the two hairpins. Most notably at position 31 in the loop 1 variant and at positions 9 and 25 in the loop 2 variant.

The close similarities in structures of the grafted peptides to the original scaffold molecule PDP-23 highlight its potential for grafting. Notably, the seven-residue epitope (T K S I P P I) is completely different in both composition and length from that of the native scaffold. The grafted epitope when inserted in PDP-23-SFTI-loop 1 extends the native loop (W H H S) whereas the grafted epitope in PDP-23-SFTI-Loop2 is shorter than the native loop (A D F P W P L G H Q). Thus, the PDP-23 scaffold can accommodate significant variation while retaining the well-defined fold in both loops. A previous study suggested sequence composition has a larger impact on the fold of grafted cyclotides rather than length of the grafts.[39] Here we chose a bioactive loop that has inherent stability given the disulfide bond support is retained. It would be interesting to explore PDP-23 using more dynamic grafts.

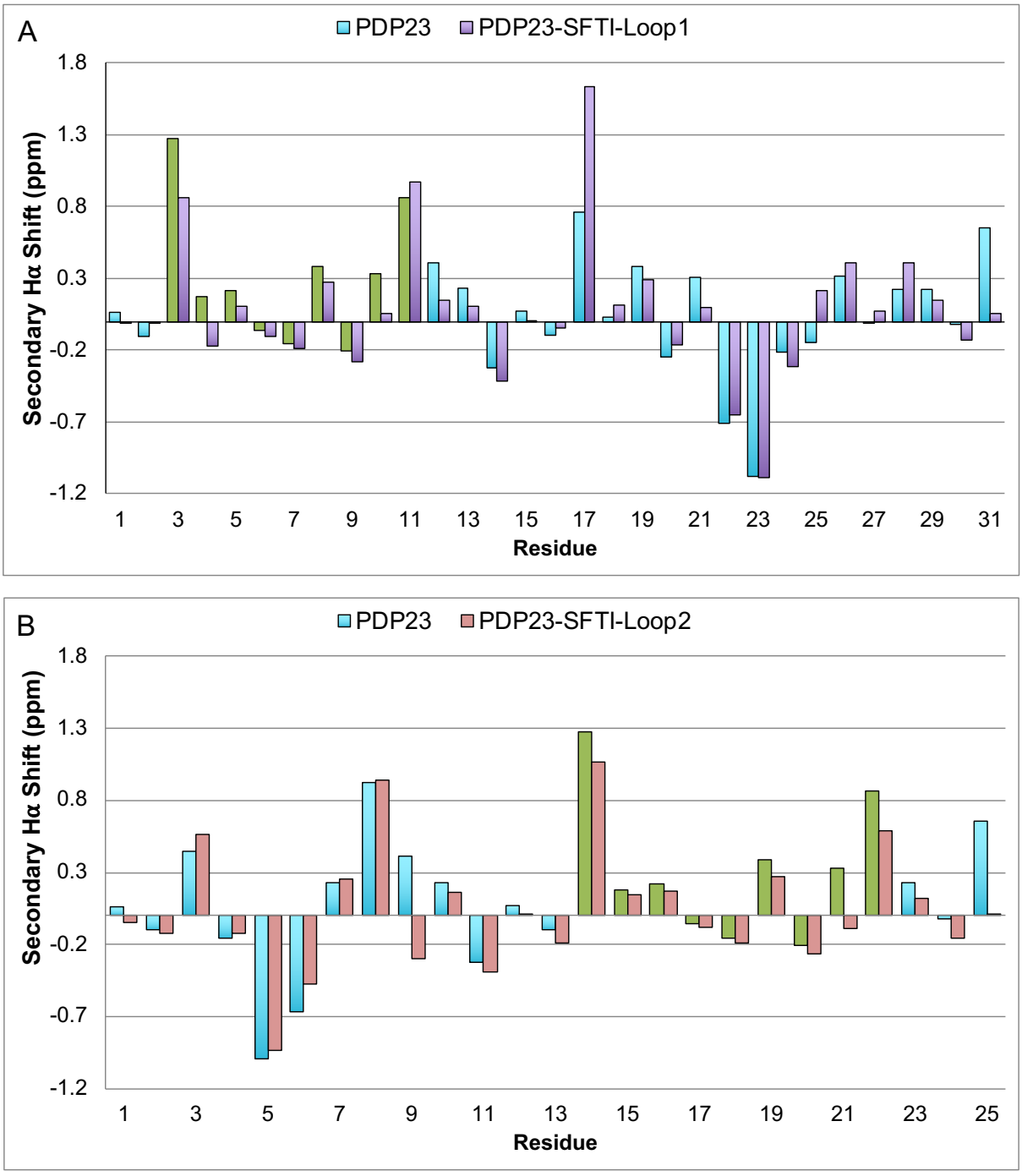

Figure 2. NMR structural analysis of native PDP23 and SFTI grafted analogues.
Hα secondary chemical shifts of SFTI grafted PDP-23 in loop 1 (A) and SFTI grafted PDP-23 in loop 2 (B) compared with native PDP-23 (presented in light blue color) and native SFTI-1. (green color).

The obtained NMR spectra for the RGD grafted peptides were of even higher quality with excellent line shape and dispersion, closely matching the data for native PDP-23. Sequential assignment using the TOCSY and NOESY NMR data was straight forward indicating a well-defined structure and the secondary shift analysis, presented in Figure 3, revealed essentially

identical chemical shifts for both RGD-containing PDP-23 analogues and native PDP-23. The native PDP-23 scaffold adopts well-defined 3D structure characterized by two anti-parallel β-sheets, each cross-braced by a single disulfide bond, and several well-defined turns. The fold is stabilized by a large number of hydrogen bonds and the cyclic backbone. Based on the Hα secondary chemical the RGD grafted PDP-23 analogues retained identical structural features, with differences only observed around the insertion of the RGD sequence.

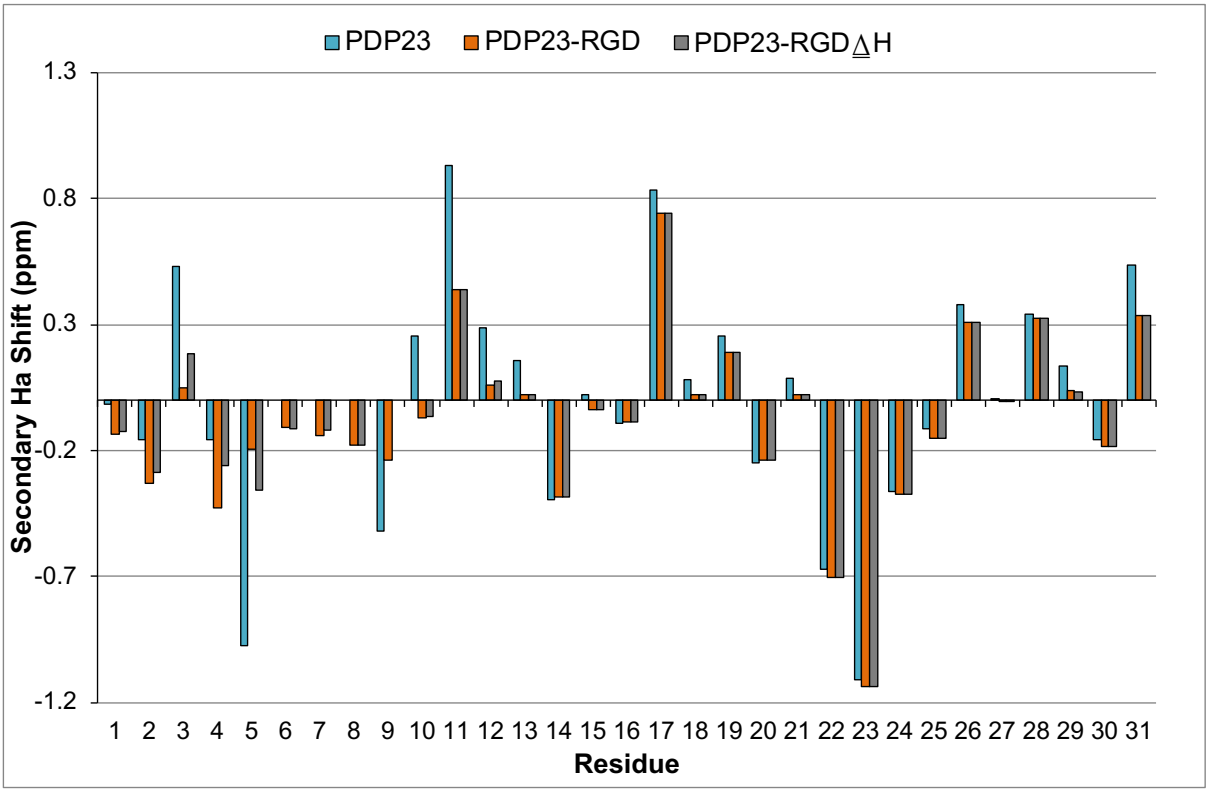

Figure 3. NMR structural analysis of native PDP-23 and RGD grafted analogues.
Hα secondary chemical shifts of RGD grafted PDP-23 analogues compared with native PDP-23. Residues 6, 7 and 8 are the inserted RGD. The second part of the native sequence has been aligned such that His6 is shown at position 9, given the insertion is between His5 and His6. The large negative secondary shift seen for His5 and His6 in native PDP-23 is related to the type I' β-turn adopted by this segment, not present with an RGD insertion.

Trypsin inhibition activity

The native PDP-23 and the SFTI grafted peptide analogues (loop 1 and loop 2) were tested for trypsin inhibition and compared to a Bowman-Birk trypsin inhibitor (BBI) from soybean (Figure 4). As expected, based on the NMR data, which suggested that the conformation of the bioactive loop of SFTI-1 was retained in our grafted variant, both analogues inhibited trypsin with an IC_{50} of ~0.8 μM. In contrast, no inhibition was observed for native PDP-23, consistent with its lack of a suitable Arg or Lys residue able to target the trypsin active site. The results confirmed that PDP-23 can accept larger grafts targeting enzyme activity. Given there was no

significant difference between the variants' activity, both loops are amenable to modifications. Interestingly, both SFTI-1 grafted peptides are less potent compared to the BBI trypsin inhibitor, and indeed to native SFTI-1, which is the smallest and most potent inhibitors of the BBI family.[10] In addition to the covalent cyclisation of the backbone in SFTI-1 and the disulfide bond, an extensive hydrogen bond network has been proposed as essential for maintaining full activity. However, it is possible to remove either the cyclic backbone[32] or disulfide bond[40] in SFTI-1 without conferring a substantial loss of activity. Given the NMR chemical shift analysis showing that the bioactive epitopes in the grafted variants are essentially identical to native SFTI-1,[32] we propose that these structural features have all been retained, thus the likely explanation for the reduced activity is that steric hindrance from the second loop in PDP-23 is preventing an efficient interaction with trypsin.

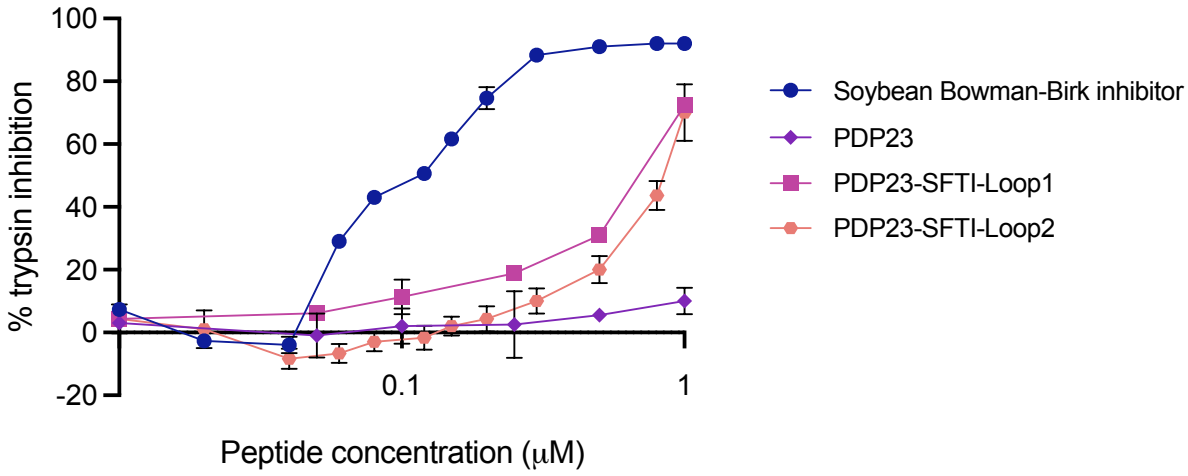

Figure 4. Inhibition of bovine trypsin by PDP-23 and SFTI grafted PDP-23.
Trypsin activity was determined in the presence of PDP23-SFTI_loop1, and PDP23-SFTI_loop1 at a range of concentrations from 0.01 to 1 μM. Soybean Bowman–Birk inhibitor was used as a positive control.

Due to the lack of trypsin in plants, it has been speculated that the potent trypsin inhibitor SFTI-1 evolved to protect against insects.[41] The majority of PDPs, including PDP-23, do not share this bioactivity, but they may still be involved in plant defense in a yet to be discovered capacity. Many proteases are attractive therapeutic targets and SFTI-1 and larger cyclic plant protease inhibitors such as MCoTI-II have been shown to be versatile scaffolds for specific targeting of these enzymes. This include the serine proteases β-tryptase and human leukocyte elastase (HLE) for the treatment of inflammatory and allergic disorders[42] and the of foot-and-mouth-disease virus (FMDV) 3C protease.[43] Although it is encouraging to see that PDP-23 is

able to host large functional grafts, for targeting of proteases scaffolds that are already native inhibitors may be more effective, due to PDP-23s more complex tertiary fold.

RGD grafted PDP-23-rhodamine conjugate toxicity and daunorubicin sensitivity

PDP-23 was considered a scaffold for drug development due to its stability, lack of toxicity, and capacity to enter cells.[19] Prior to the RGD grafted PDP-23-rhodamine conjugate toxicity and daunorubicin sensitivity determination study, a cytotoxicity study was performed to screen the cytotoxicity of the grafted peptides at different concentrations using an MTT assay. No peptide variant showed any significant toxicity again the human HeLa cell line culture (Supporting Information Figure 6).

In our previous study PDP-23 D28K-rhodamine was shown to sensitize the cell line KB V-1, which is otherwise highly resistant to chemotherapeutics.[19] The resistance is due to that KB-V-1, unlike its parent cell line KB-3-1, overexpresses the drug efflux pump P-gp, thereby minimizing intracellular concentrations of toxic drug. The dye 5/6-carboxy-tetramethyl-rhodamine is also a substrate of P-gp, but when attached to PDP-23 is too large to be pumped out of the cell, consequently acting as a P-gp inhibitor. Thus, when dosed together with chemotherapeutics the conjugate is able to reverse resistance back to the levels of KB-3-1. Here, we tested the two analogues of RGD grafted PDP-23 as D28K-rhodamine conjugates for inhibition of P-gp by exposing it in combination with the well characterized chemotherapeutic, and known substrate of P-gp, daunorubicin. None of the analogues had any significant effect on the sensitive KB-3-1 cells when dosed in combination with daunorubicin (Figure 5). In contrast, both RGD grafted PDP-23 D28K-rhodamine conjugates in combination with daunorubicin induced significantly increased cell death in the resistant cells (KB-V-1). Comparison between RGD grafted PDP-23 variants and PDP-23 revealed that the grafted conjugates could significantly increase the cell death at lower concentration (10 μM), whereas the PDP-23 conjugate significantly increased the cell death only at the high dose (30 μM). Despite the similarity of the structure for both analogues observed in NMR data analysis, the analogue in which the RGD sequence was inserted between the His5-His6 residues in loop 1, rather than replacing His6, showed significantly higher potency at the lowest dose ($p>0.05$). These findings are consistent with what was observed for the classical P-gp inhibitor verapamil.[44] RGD-binding integrins are highly expressed in a variety of cancer cells, where they play a critical role in pathophysiological processes that are important for the development of cancer. Peptides containing RGD sequences have been widely used as a molecular vector

that targets the tumor-associated cells expressing $\alpha_V\beta_3$ receptors with to deliver the chemotherapeutics to the malignant tissues.[25, 45] The conformation of the RGD motif strongly influence integrin binding, and the difference in activity between the two RGD grafted variants is likely due to a conformational difference modulating the strength of interaction. Binding to integrins will increase the concentration at the cell membrane and consequently, as a result of endocytosis, the intracellular concentration leading to the observed increase in activity.

Despite the advancement in therapies employed for cancer treatments, chemotherapy remains the most widely used cancer treatment option today. The invasion and spread of cancers caused by drug resistance account for over 90% of chemotherapy failures.[46] The important role of P-gp in multidrug resistance is well established,[44] and KB-V-1 cells are commonly used as models for this type of resistance.[19, 47] Typically, the strategy using peptides as carriers by conjugating to small molecule drugs is focused on overcoming common small molecule issues, including poor solubility, metabolism, and off-target effects due to unfavorable distribution. Preclinical and clinical studies have been conducted for peptide–drug conjugates such as gonadotropin-releasing hormone conjugated to doxorubicin for the treatment of ovarian and endometrial cancers,[48] paclitaxel–angiopep-2 conjugate for the treatment of glioblastoma, lung and ovarian cancers[49] as well as radiolabeled somatostatin analogs, like [DOTA, Tyr3]octreotide and [DOTA, Tyr3]octreotate treatment modality for somatostatin receptor-positive tumors for targeted radiotherapy.[50] Consistent with the results of this study, it has shown a paclitaxel–angiopep-2 conjugate allows paclitaxel to cross the blood–brain barrier entering the brain to a greater extent than paclitaxel and importantly prevents efflux by P-gp expressed on the blood-brain barrier.[49]

A

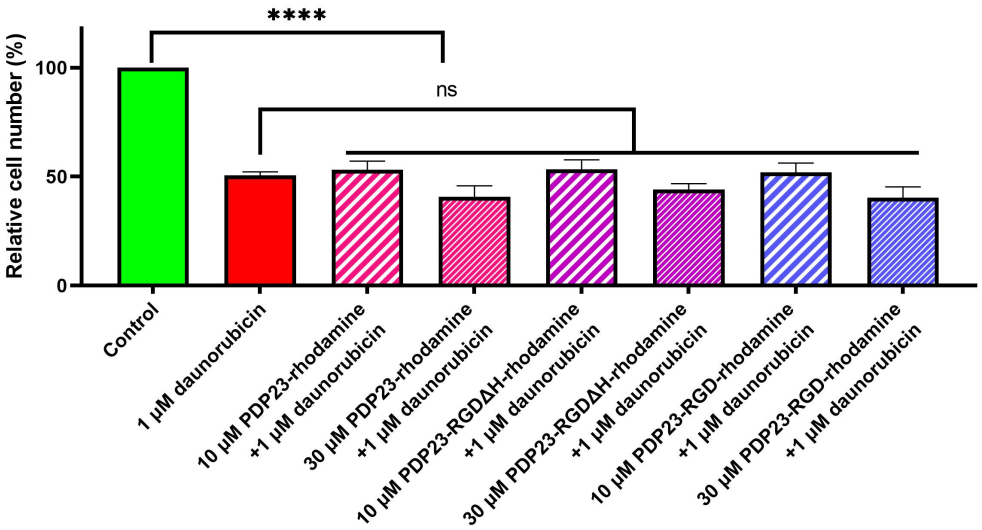
****
ns
Relative cell number (%)
100
50
0
Control
1 μM daunorubicin
10 μM PDP23-rhodamine +1 μM daunorubicin
30 μM PDP23-rhodamine +1 μM daunorubicin
10 μM PDP23-RGDΔH-rhodamine +1 μM daunorubicin
30 μM PDP23-RGDΔH-rhodamine +1 μM daunorubicin
10 μM PDP23-RGD-rhodamine +1 μM daunorubicin
30 μM PDP23-RGD-rhodamine +1 μM daunorubicin

B

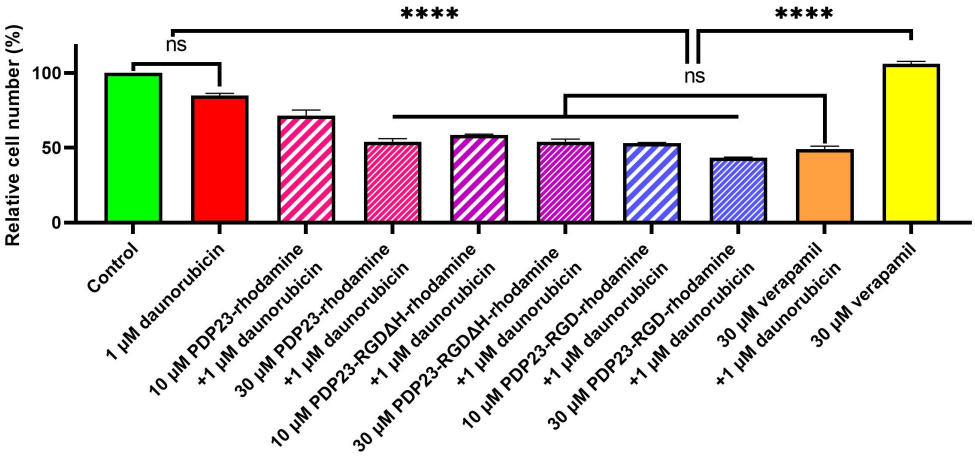
****
****
ns
ns
Relative cell number (%)
100
50
0
Control
1 μM daunorubicin
10 μM PDP23-rhodamine +1 μM daunorubicin
30 μM PDP23-rhodamine +1 μM daunorubicin
10 μM PDP23-RGDΔH-rhodamine +1 μM daunorubicin
30 μM PDP23-RGDΔH-rhodamine +1 μM daunorubicin
10 μM PDP23-RGD-rhodamine +1 μM daunorubicin
30 μM PDP23-RGD-rhodamine +1 μM daunorubicin
30 μM verapamil +1 μM daunorubicin
30 μM verapamil

C

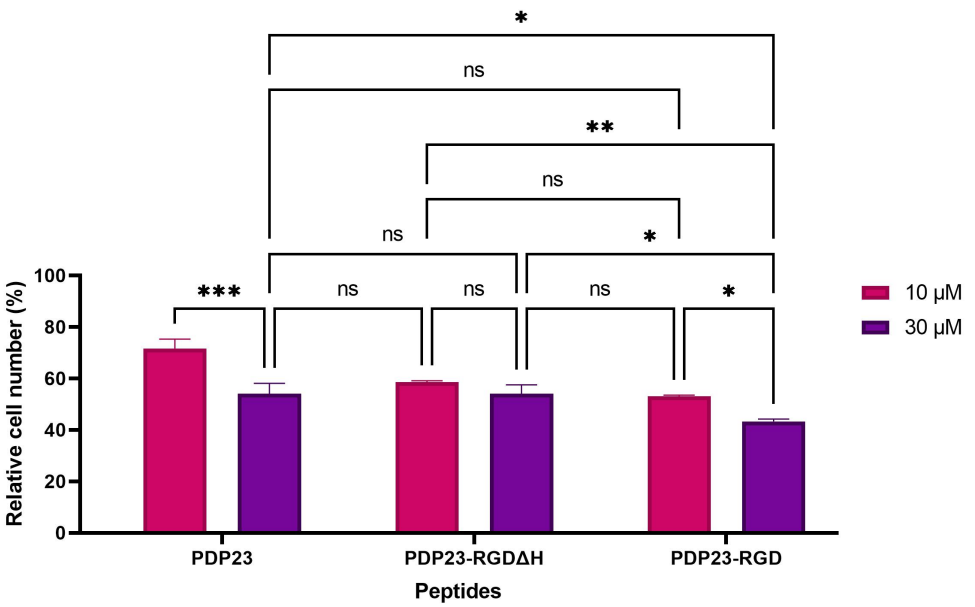
*
ns
**
ns
ns
*
***
ns
ns
ns
*
Relative cell number (%)
100
80
60
40
20
0
10 μM
30 μM
PDP23
PDP23-RGDΔH
PDP23-RGD
Peptides

Figure 5. Cell toxicity and daunorubicin sensitivity determination.
Comparison of toxicity of a single concentration of daunorubicin (1 μM) in sensitive KB-3-1 (A) and resistant KB-V-1 (B) cells, in the presence or absence of the PDP-23 and RGD grafted PDP-23-rhodamine conjugates. Controls for P-gp inhibition include 30 μM verapamil supplemented with 1 μM daunorubicin and daunorubicin alone. Untreated cells and cells treated with verapamil alone were included as negative controls. (C) Comparison of grafted PDPs and PDP-23 in KB-V-1 cells.

Conclusion

In this study we investigated how tolerant the PDP-23 scaffold is for molecular grafting and whether it can be used to host bioactive epitopes mediating enzyme inhibition (SFTI-1) and protein-protein interactions (RGD). All variants were readily assembled, cyclized and folded using chemical synthesis. The quality of NMR data recorded in water were poor, with broad lines suggesting partial aggregation and intermediate conformational exchange. We attribute this to the grafts destabilizing the dimer formed by native PDP-23 in aqueous conditions. However, addition of 20% ACN improved the data, allowing full assignment and comparison to native PDP-23, which under these conditions adopts a highly structured monomer. The similarities in chemical shifts of the grafted analogues to both the native PDP-23 and, where relevant, native SFTI indicate that the structure of both the scaffold and the graft were fully retained. Both SFTI grafted PDP-23 variants demonstrated trypsin inhibition activity not seen for native PDP-23. Furthermore, PDP-23 grafted with RGD was investigated as a potential scaffold for targeted delivery of small molecule therapeutics. The RGD grafted PDP-23-rhodamine conjugate did not significantly increase cell death in the daunorubicin-sensitive KB-3-1 cells in the presence of daunorubicin. However, the addition of RGD-grafted PDP-23 D28K -rhodamine in conjunction with daunorubicin significantly increased cell death in the highly resistant cell line KB V-1 in a dose-dependent manner, indicating the restoration of chemotherapy sensitivity by inhibition of the efflux pump P-gp. Importantly, this effect was significantly enhanced compared to native PDP-23 lacking the RGD sequence, suggesting the ability to bind to integrin receptors in KB-V-1 cells leads to an increase in cell uptake and increased intracellular concentration. This study demonstrates the application of PDP-23 as a drug scaffold for chemotherapeutics targeting drug-resistant cancer cells.

In conclusion, this study highlights that PDP-23 can provide a versatile scaffold for grafting bioactive sequences of multiple lengths and at multiple positions. Given the ability of PDP-23 to adopt different conformations under different conditions and penetrate cells, this type of scaffold might offer significant advantages over other commonly used rigid variants.

Acknowledgements

This work was supported by the Australian Research Council (DP190102058). The authors would like to thank Honorary Professor Rodney Minchin, School of Biomedical Sciences, the University of Queensland for generously providing the KB-3-1 and KB-V-1 cells.

References

(1) Craik, D. J.; Fairlie, D. P.; Liras, S.; Price, D. The future of peptide-based drugs. *Chemical biology & drug design* **2013**, *81* (1), 136-147.
(2) Wang, L.; Wang, N.; Zhang, W.; Cheng, X.; Yan, Z.; Shao, G.; Wang, X.; Wang, R.; Fu, C. Therapeutic peptides: Current applications and future directions. *Signal Transduction and Targeted Therapy* **2022**, *7* (1), 48.
(3) Li, C. M.; Haratipour, P.; Lingeman, R. G.; Perry, J. J. P.; Gu, L.; Hickey, R. J.; Malkas, L. H. Novel peptide therapeutic approaches for cancer treatment. *Cells* **2021**, *10* (11), 2908.
(4) Bhardwaj, G.; Mulligan, V. K.; Bahl, C. D.; Gilmore, J. M.; Harvey, P. J.; Cheneval, O.; Buchko, G. W.; Pulavarti, S. V. S. R. K.; Kaas, Q.; Eletsky, A.; et al. Accurate de novo design of hyperstable constrained peptides. *Nature* **2016**, *538* (7625), 329-335, Article.
(5) Muttenthaler, M.; King, G. F.; Adams, D. J.; Alewood, P. F. Trends in peptide drug discovery. *Nature reviews Drug discovery* **2021**, *20* (4), 309-325.
(6) Zhang, J.; Yuan, J.; Li, Z.; Fu, C.; Xu, M.; Yang, J.; Jiang, X.; Zhou, B.; Ye, X.; Xu, C. Exploring and exploiting plant cyclic peptides for drug discovery and development. *Medicinal Research Reviews* **2021**, *41* (6), 3096-3117.
(7) Tyler, T. J.; Durek, T.; Craik, D. J. Native and Engineered Cyclic Disulfide-Rich Peptides as Drug Leads. *Molecules* **2023**, *28* (7), 3189.
(8) Clark, R. J.; Daly, N. L.; Craik, D. J. Structural plasticity of the cyclic-cystine-knot framework: implications for biological activity and drug design. *Biochemical Journal* **2006**, *394* (1), 85-93.
(9) Gunasekera, S.; Foley, F. M.; Clark, R. J.; Sando, L.; Fabri, L. J.; Craik, D. J.; Daly, N. L. Engineering stabilized vascular endothelial growth factor-A antagonists: synthesis, structural characterization, and bioactivity of grafted analogues of cyclotides. *Journal of medicinal chemistry* **2008**, *51* (24), 7697-7704.
(10) Luckett, S.; Garcia, R. S.; Barker, J.; Konarev, A. V.; Shewry, P.; Clarke, A.; Brady, R. High-resolution structure of a potent, cyclic proteinase inhibitor from sunflower seeds. *Journal of molecular biology* **1999**, *290* (2), 525-533.
(11) de Veer, S. J.; White, A. M.; Craik, D. J. Sunflower trypsin Inhibitor-1 (SFTI-1): sowing seeds in the fields of chemistry and biology. *Angewandte Chemie International Edition* **2021**, *60* (15), 8050-8071.
(12) Sable, R.; Durek, T.; Taneja, V.; Craik, D. J.; Pallerla, S.; Gauthier, T.; Jois, S. Constrained cyclic peptides as immunomodulatory inhibitors of the CD2: CD58 protein–protein interaction. *ACS chemical biology* **2016**, *11* (8), 2366-2374.
(13) Gunasekera, S.; Fernandes-Cerqueira, C. t.; Wennmalm, S.; Wähämaa, H.; Sommarin, Y.; Catrina, A. I.; Jakobsson, P.-J.; Göransson, U. Stabilized cyclic peptides as scavengers of autoantibodies: neutralization of anticitrullinated protein/peptide antibodies in rheumatoid arthritis. *ACS Chemical Biology* **2018**, *13* (6), 1525-1535.
(14) Swedberg, J. E.; Li, C. Y.; De Veer, S. J.; Wang, C. K.; Craik, D. J. Design of potent and selective cathepsin G inhibitors based on the sunflower trypsin inhibitor-1 scaffold. *Journal of Medicinal Chemistry* **2017**, *60* (2), 658-667.

(15) Jendrny, C.; Beck-Sickinger, A. G. Inhibition of kallikrein-related peptidases 7 and 5 by grafting serpin reactive-center loop sequences onto sunflower trypsin inhibitor-1 (SFTI-1). *ChemBioChem* **2016**, *17* (8), 719-726.
(16) Li, C. Y.; Yap, K.; Swedberg, J. E.; Craik, D. J.; de Veer, S. J. Binding loop substitutions in the cyclic peptide SFTI-1 generate potent and selective chymase inhibitors. *Journal of Medicinal Chemistry* **2019**, *63* (2), 816-826.
(17) Durek, T.; Cromm, P. M.; White, A. M.; Schroeder, C. I.; Kaas, Q.; Weidmann, J.; Ahmad Fuaad, A.; Cheneval, O.; Harvey, P. J.; Daly, N. L. Development of novel melanocortin receptor agonists based on the cyclic peptide framework of sunflower trypsin inhibitor-1. *Journal of medicinal chemistry* **2018**, *61* (8), 3674-3684.
(18) Elliott, A. G.; Franke, B.; Armstrong, D. A.; Craik, D. J.; Mylne, J. S.; Rosengren, K. J. Natural structural diversity within a conserved cyclic peptide scaffold. *Amino Acids* **2017**, *49* (1), 103-116.
(19) Payne, C. D.; Franke, B.; Fisher, M. F.; Hajiaghaalipour, F.; McAleese, C. E.; Song, A.; Eliasson, C.; Zhang, J.; Jayasena, A. S.; Vadlamani, G. A chameleonic macrocyclic peptide with drug delivery applications. *Chemical science* **2021**, *12* (19), 6670-6683.
(20) Payne, C. D.; Vadlamani, G.; Hajiaghaalipour, F.; Muhammad, T.; Fisher, M. F.; Andersson, H. S.; Göransson, U.; Clark, R. J.; Bond, C. S.; Mylne, J. S. Solution NMR and racemic crystallography provide insights into a novel structural class of cyclic plant peptides. *RSC chemical biology* **2021**, *2* (6), 1682-1691.
(21) Jayasena, A. S.; Fisher, M. F.; Panero, J. L.; Secco, D.; Bernath-Levin, K.; Berkowitz, O.; Taylor, N. L.; Schilling, E. E.; Whelan, J.; Mylne, J. S. Stepwise evolution of a buried inhibitor peptide over 45 My. *Molecular Biology and Evolution* **2017**, *34* (6), 1505-1516.
(22) Zorko, M.; Jones, S.; Langel, Ü. Cell-penetrating peptides in protein mimicry and cancer therapeutics. *Advanced Drug Delivery Reviews* **2022**, *180*, 114044.
(23) Khalily, M. P.; Soydan, M. Peptide-based diagnostic and therapeutic agents: Where we are and where we are heading? *Chemical Biology & Drug Design* **2023**, *101* (3), 772-793.
(24) Zhang, Q.; Liu, N.; Wang, J.; Liu, Y.; Wang, K.; Zhang, J.; Pan, X. The Recent Advance of Cell-Penetrating and Tumor-Targeting Peptides as Drug Delivery Systems Based on Tumor Microenvironment. *Molecular Pharmaceutics* **2023**.
(25) Danhier, F.; Le Breton, A.; Préat, V. r. RGD-based strategies to target alpha (v) beta (3) integrin in cancer therapy and diagnosis. *Molecular pharmaceutics* **2012**, *9* (11), 2961-2973.
(26) Pierschbacher, M. D.; Ruoslahti, E. Cell attachment activity of fibronectin can be duplicated by small synthetic fragments of the molecule. *Nature* **1984**, *309* (5963), 30-33.
(27) Wüthrich, K. NMR with proteins and nucleic acids. *Europhysics News* **1986**, *17* (1), 11-13.
(28) Schroeder, C. I.; Rosengren, K. J. Three-dimensional structure determination of peptides using solution nuclear magnetic resonance spectroscopy. *Snake and Spider Toxins: Methods and Protocols* **2020**, 129-162.
(29) Wishart, D. S.; Bigam, C. G.; Holm, A.; Hodges, R. S.; Sykes, B. D. 1 H, 13 C and 15 N random coil NMR chemical shifts of the common amino acids. I. Investigations of nearest-neighbor effects. *Journal of biomolecular NMR* **1995**, *5* (1), 67-81.
(30) Zhang, J.; Payne, C. D.; Pouvreau, B.; Schaefer, H.; Fisher, M. F.; Taylor, N. L.; Berkowitz, O.; Whelan, J.; Rosengren, K. J.; Mylne, J. S. An ancient peptide family buried within vicilin precursors. *ACS Chemical Biology* **2019**, *14* (5), 979-993.
(31) Van Meerloo, J.; Kaspers, G. J.; Cloos, J. Cell sensitivity assays: the MTT assay. In *Cancer cell culture*, Springer, 2011; pp 237-245.
(32) Korsinczky, M. L.; Schirra, H. J.; Rosengren, K. J.; West, J.; Condie, B. A.; Otvos, L.; Anderson, M. A.; Craik, D. J. Solution structures by 1H NMR of the novel cyclic trypsin inhibitor SFTI-1 from sunflower seeds and an acyclic permutant. *Journal of molecular biology* **2001**, *311* (3), 579-591.
(33) Mas-Moruno, C.; Rechenmacher, F.; Kessler, H. Cilengitide: the first anti-angiogenic small molecule drug candidate. Design, synthesis and clinical evaluation. *Anti-Cancer Agents in Medicinal Chemistry (Formerly Current Medicinal Chemistry-Anti-Cancer Agents)* **2010**, *10* (10), 753-768.

(34) Kapp, T. G.; Rechenmacher, F.; Neubauer, S.; Maltsev, O. V.; Cavalcanti-Adam, E. A.; Zarka, R.; Reuning, U.; Notni, J.; Wester, H.-J.; Mas-Moruno, C. A comprehensive evaluation of the activity and selectivity profile of ligands for RGD-binding integrins. *Scientific reports* **2017**, *7* (1), 39805.
(35) Conibear, A. C.; Bochen, A.; Rosengren, K. J.; Stupar, P.; Wang, C.; Kessler, H.; Craik, D. J. The Cyclic Cystine Ladder of Theta-Defensins as a Stable, Bifunctional Scaffold: A Proof-of-Concept Study Using the Integrin-Binding RGD Motif. *ChemBioChem* **2014**, *15* (3), 451-459.
(36) Knappe, T. A.; Manzenrieder, F.; Mas-Moruno, C.; Linne, U.; Sasse, F.; Kessler, H.; Xie, X.; Marahiel, M. A. Introducing lasso peptides as molecular scaffolds for drug design: engineering of an integrin antagonist. *Angewandte Chemie International Edition* **2011**, *50* (37), 8714-8717.
(37) Bergonzini, C.; Kroese, K.; Zweemer, A. J.; Danen, E. H. Targeting integrins for cancer therapy-disappointments and opportunities. *Frontiers in Cell and Developmental Biology* **2022**, *10*.
(38) Gu, Y.; Dong, B.; He, X.; Qiu, Z.; Zhang, J.; Zhang, M.; Liu, H.; Pang, X.; Cui, Y. The challenges and opportunities of αvβ3-based therapeutics in cancer: from bench to clinical trials. *Pharmacological Research* **2023**, 106694.
(39) Wong, C. T.; Rowlands, D. K.; Wong, C. H.; Lo, T. W.; Nguyen, G. K.; Li, H. Y.; Tam, J. P. Orally active peptidic bradykinin B1 receptor antagonists engineered from a cyclotide scaffold for inflammatory pain treatment. *Angewandte Chemie International Edition* **2012**, *51* (23), 5620-5624.
(40) Korsinczky, M. L.; Clark, R. J.; Craik, D. J. Disulfide bond mutagenesis and the structure and function of the head-to-tail macrocyclic trypsin inhibitor SFTI-1. *Biochemistry* **2005**, *44* (4), 1145-1153.
(41) Elliott, A. G.; Delay, C.; Liu, H.; Phua, Z.; Rosengren, K. J.; Benfield, A. H.; Panero, J. L.; Colgrave, M. L.; Jayasena, A. S.; Dunse, K. M.; et al. Evolutionary origins of a bioactive peptide buried within preproalbumin. *Plant Cell* **2014**, *26* (3), 981-995.
(42) Thongyoo, P.; Bonomelli, C.; Leatherbarrow, R. J.; Tate, E. W. Potent inhibitors of β-tryptase and human leukocyte elastase based on the MCoTI-II scaffold. *Journal of medicinal chemistry* **2009**, *52* (20), 6197-6200.
(43) Thongyoo, P.; Roqué-Rosell, N.; Leatherbarrow, R. J.; Tate, E. W. Chemical and biomimetic total syntheses of natural and engineered MCoTI cyclotides. *Organic & biomolecular chemistry* **2008**, *6* (8), 1462-1470.
(44) Nanayakkara, A. K.; Follit, C. A.; Chen, G.; Williams, N. S.; Vogel, P. D.; Wise, J. G. Targeted inhibitors of P-glycoprotein increase chemotherapeutic-induced mortality of multidrug resistant tumor cells. *Scientific reports* **2018**, *8* (1), 1-18.
(45) Ludwig, B. S.; Kessler, H.; Kossatz, S.; Reuning, U. RGD-binding integrins revisited: how recently discovered functions and novel synthetic ligands (re-) shape an ever-evolving field. *Cancers* **2021**, *13* (7), 1711.
(46) Bukowski, K.; Kciuk, M.; Kontek, R. Mechanisms of multidrug resistance in cancer chemotherapy. *International journal of molecular sciences* **2020**, *21* (9), 3233.
(47) Galmarini, C. M. P-glycoprotein expression by cancer cells affects cell cytotoxicity and cell-cycle perturbations induced by six chemotherapeutic drugs. *Journal of Experimental Therapeutics and Oncology* **2002**, *2* (3), 146-152.
(48) Westphalen, S.; Kotulla, G.; Kaiser, F.; Krauss, W.; Werning, G.; Elsasser, H. P.; Nagy, A.; Schulz, K.-D.; Grundker, C.; Schally, A. V. Receptor mediated antiproliferative effects of the cytotoxic LHRH agonist AN-152 in human ovarian and endometrial cancer cell lines. *International journal of oncology* **2000**, *17* (5), 1063-1072.
(49) Regina, A.; Demeule, M.; Che, C.; Lavallee, I.; Poirier, J.; Gabathuler, R.; Béliveau, R.; Castaigne, J. P. Antitumour activity of ANG1005, a conjugate between paclitaxel and the new brain delivery vector Angiopep-2. *British journal of pharmacology* **2008**, *155* (2), 185-197.
(50) De Jong, M.; Valkema, R.; Jamar, F.; Kvols, L. K.; Kwekkeboom, D. J.; Breeman, W. A.; Bakker, W. H.; Smith, C.; Pauwels, S.; Krenning, E. P. Somatostatin receptor-targeted radionuclide therapy of tumors: preclinical and clinical findings. In *Seminars in nuclear medicine*, 2002; Elsevier: Vol. 32, pp 133-140.